Age Classification of Evacuees at Times of Disaster Using a Vibration Sensor

Toru YAMASHITA*, Futoshi ASANO* and Kazuhiro NAKADAI †
* Faculty of Informatics, Kogakuin University, Tokyo, Japan
E-mail: asano@cc.kogakuin.ac.jp
† Honda Research Institute Japan, Saitama, Japan

***Abstract*—In this study, a method to detect children evacuating from a building at the time of a disaster using a vibration sensor is proposed. The features for detection are obtained using linear prediction, which is suitable for analyzing resonance phenomena such as speech. Subsequently, the extracted features are used in the linear discrimination analysis to discriminate between children and adults. Experimental results with 40 subjects show that the detection rate was approximately 80% in the test environment.**

I. Introduction

At the time of a disaster, evacuees may be left in buildings. When a blackout occurs, it would be difficult for them to find an evacuation route by themselves. In particular, it is necessary to detect children who have lost sight of their parents and to take appropriate actions, such as sending a rescue team. Methods have been developed to estimate the status of evacuees, such as walking direction or speed, for the assistance of evacuation, using vibration sensors [1], [2]. In previous work [3], a method was proposed to classify the weights of subjects by applying linear prediction (LP) [4] to the observation of vibration sensors. In the present study, the idea of the above weight classification was applied to indirect age classification (children/adults). A new feature appropriate for age classification was introduced and verified. Subsequently, an evaluation experiment with 40 subjects was conducted in a real environment. By using the proposed method, it is possible to detect children during an evacuation, and the efficiency of rescuing them is expected to improve.

In a similar study, Pan *et al*. [5] proposed a method to identify the members of a small group (e.g., 10 people) by using vibration sensors. In their method, differences in footsteps for each subject were extracted using the fast Fourier transform (FFT) spectrum with high resolution. However, in this study, the simplified features of footsteps, i.e., the pole distributions in the LP spectrum, were utilized to suppress the individual differences and to classify the subjects according to their age.

As an alternative approach, the use of visual information for age classification is also proposed [6]. During a blackout, visual information appropriate for age classification may not be available. Moreover, in evacuation during disasters, children may be lost while they are using washrooms or dressing rooms. The use of cameras in these private areas is usually restricted. By using vibration sensors, the problem of privacy can be avoided.

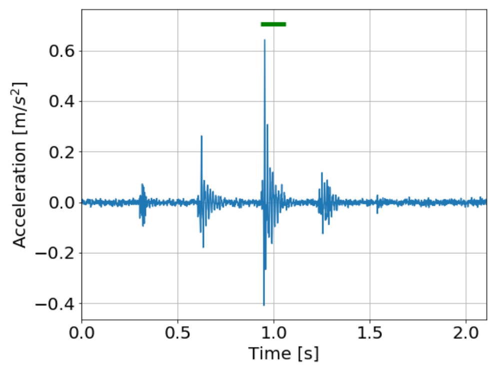

Fig. 1. Example of the observation.

II. Sensors and observations

In this study, the MVP-RF10-AC-500 vibration sensor (MicroStone) was used. It has dimensions of 45 × 45 × 18 mm and weighs 50 g. It can measure acceleration in the x- and y-directions (horizontal) and the z-direction (vertical). In this study, the acceleration in the z-direction was used because the signal-to-noise ratio (SNR) was higher than those in the x- and y-directions [7]. The sampling rate was 1 kHz.

Fig. 1 shows an example of the observation used in the experiments described in Section 5. In this study, a single footstep, which is generated when the foot was the closest to the sensor (where the SNR was expected to be the highest) while the subjects passed by the sensor, was used for the classification. In Fig. 1, the frame corresponding to a single footstep is indicated by the green line shown at the top of the figure. The length of the frame is 128 points (128 ms).

III. Features

The waveform generated by a footstep was modeled by LP, and its parameters were utilized as features for classification. The results of the preliminary experiments using a plastic hammer and those using real footsteps are shown.

A. Feature extraction

In LP, the observation $y(n)$ is modeled as

$$\hat{y}(n) = -\sum_{k=1}^{M} a_k y(n-k) \tag{1}$$

where a_k is the LP coefficient (LPC). The symbol M is the model order. The LPCs are determined by minimizing the following prediction error:

$$v(n) = y(n) - \hat{y}(n) \tag{2}$$

When $v(n)$ is regarded as the system input, the transfer function $H(z)$ between input $v(n)$ and output $y(n)$ can be written as

$$\begin{aligned} H(z) &= \frac{1}{\sum_{k=0}^{M} a_k z^{-k}} \\ &= \frac{z^M}{\prod_{m=1}^{M/2}(z - r_m e^{j\theta_m})(z - r_m e^{-j\theta_m})} \end{aligned} \tag{3}$$

where r_m and θ_m are the radius and the angle of the poles of $H(z)$, respectively. The relation between the resonant frequency f_m and angle θ_m is expressed as

$$f_m = f_s \cdot \frac{\theta_m}{2\pi} \tag{4}$$

where f_s indicates the sampling frequency. From this, it can be seen that θ_m is larger when the resonant frequency is higher. On the other hand, when r_m is close to 1, the corresponding resonance becomes sharper. Thus, in this study, the parameters (r_m, θ_m), which reflect the status of the resonance, are utilized as the features.

$$\boldsymbol{x} = [r_1, \theta_1]^T \tag{5}$$

where it is assumed that the poles are sorted in the descending order of $\{r_m\}$, that is, $r_1 > \cdots > r_{M/2}$.

B. Preliminary experiments using a hammer

The validity of the features used for the classification was examined by a simplified experiment using a plastic hammer. Fig. 2 shows the scene of the experiment. A point on the floor with a distance of 0.5 m from the sensor was hit by a plastic hammer. The head of the hammer was dropped freely from a height of 7 cm, while the grip was fixed so that the hitting force was constant. Two types of hammer head with weights of 567 and 1452 g were used so that the ratio of weight was approximately 1:3. This is because the ratio of the weight of the children and the adults participating in the experiment described in Section V was approximately 1:3 (20:60 kg).

Fig. 3 shows the LP spectrum obtained by substituting $z = \exp(j\omega)$ into (3). Fig. 4 shows the corresponding pole distribution. The red circle shows the pole location (r_1, θ_1) with the largest radius. These results show that the resonant frequency was lower for the hammer with a heavy head. This is analogous to the natural frequency of the vibration system being lower for the case with a heavier mass.

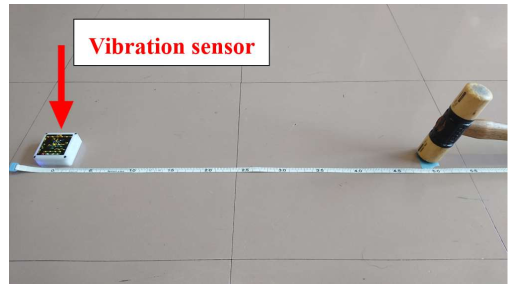

Fig. 2. Scene of the preliminary experiment using a hammer.

C. Experiment with real footsteps

An experiment similar to that described in Section III-B was conducted with real footsteps. The same point of the floor was hit by the foot of two humans with weights 18 kg and 66 kg. Figs. 5 and 6 show the LP spectrum and the pole distribution, respectively. A tendency similar to Section III-B, i.e., the resonant frequency being lower for heavier weights, was observed. Thus, the results presented in Sections III-B and III-C confirm the validity of employing the features proposed in Section III-A for the classification of weights.

IV. Classifier

For classification, a linear classifier based on the probabilistic generative model [8], often called “linear discriminant analysis” (LDA), was used. The posterior probability for class C_1 for discriminating classes C_1 and C_2 is given by

$$\begin{aligned} p(C_1|\boldsymbol{x}) &= \frac{p(\boldsymbol{x}|C_1)p(C_1)}{p(\boldsymbol{x}|C_1)p(C_1)+p(\boldsymbol{x}|C_2)p(C_2)} \\ &= \sigma(\boldsymbol{w}^T\boldsymbol{x}+w_0) \end{aligned} \tag{6}$$

where σ (a) denotes the logistic sigmoid function:

$$\sigma(a) = \frac{1}{1+\exp(-a)} \tag{7}$$

The coefficients $\boldsymbol{w}$ and w_0 are given by

$$\boldsymbol{w} = \boldsymbol{\Sigma}^{-1}(\boldsymbol{\mu}_1 - \boldsymbol{\mu}_2) \tag{8}$$

$$w_0 = \frac{1}{2}\boldsymbol{\mu}_2^T\boldsymbol{\Sigma}^{-1}\boldsymbol{\mu}_2 - \frac{1}{2}\boldsymbol{\mu}_1^T\boldsymbol{\Sigma}^{-1}\boldsymbol{\mu}_1 + \log\frac{p(C_1)}{p(C_2)} \tag{9}$$

In LDA, the data $\boldsymbol{x}$ belonging to C_k are assumed to have a normal distribution with the mean $\boldsymbol{\mu}_k$ and covariance matrix $\boldsymbol{\Sigma}$. The covariance matrix $\boldsymbol{\Sigma}$ is assumed to be common to two classes. In this study, classes C_1 and C_2 correspond to the children and adults, respectively.

V. Experiment

A. Condition

The experiments were conducted in a building at Kogakuin University. Fig.7 shows the scene of the experiments. The floor of the building consists of stone tiles. The subjects

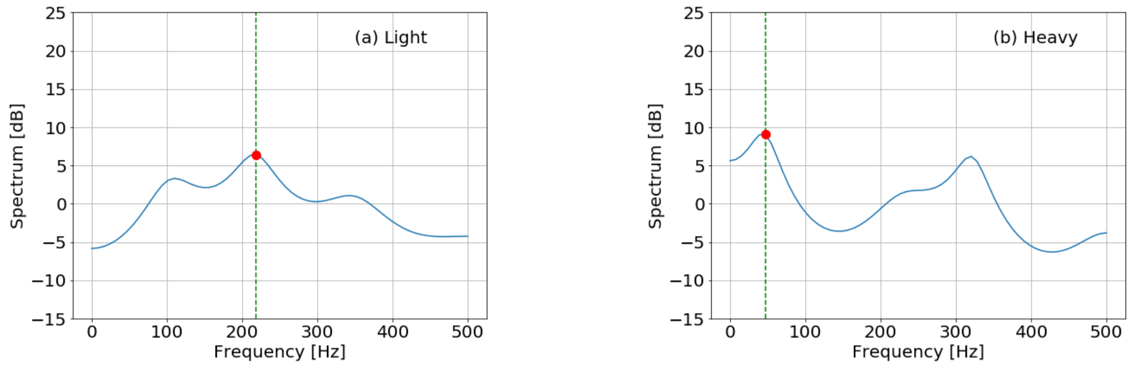

Fig. 3. Linear prediction spectrum for the preliminary experiment using a hammer: (a) light hammer head and (b)heavy hammer head.

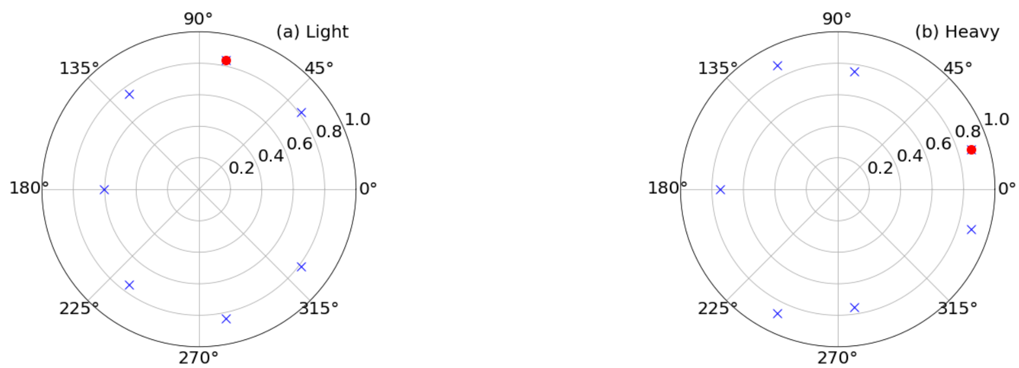

Fig. 4. Distribution of poles of the linear prediction transfer function for the preliminary experiment using a hammer: (a) light hammer head and (b)heavy hammer head. The red circle shows the pole with the largest radius.

were instructed to walk or run along the white straight-line marker. The vibration sensor was located in the middle of the marker at a distance of 20 cm. The walking/running speed was determined by each subject and was not regulated. The resultant average speed was 1.19 m/s for walking and 2.47 m/s for running. The number of subjects was 40 (20 children and 20 adults). Fig.8 shows the distribution of the ages and weights of the subjects.

B. Results

Fig. 9 shows the distribution of the features. The blue circles and the red squares indicate the features of the children and adults, respectively. The lateral and horizontal axes correspond to f_1 and r_1, respectively. The blue and red regions correspond to the area in which the posterior probabilities $p(C_1|\boldsymbol{x})$ and $p(C_2|\boldsymbol{x})$ exceed 0.5, respectively. The ellipses are equal probability ellipses for $2\times$ standard deviation. The figure shows that the features for the adults concentrate at approximately 50 Hz for running and 100 Hz for walking. On the other hand, the features for children are scattered at higher frequencies. Thus, children and adults can be classified in the feature space. The reason for the resonant frequency being lower for running is considered to be that the weight of the subject is concentrated on one foot for running while the weight is distributed on two feet for walking.

Fig.10 shows the accuracy of the classification for different prediction orders M. The accuracy was obtained by cross-validation with 10 splits. The blue line indicates the case of the proposed method. For comparison, the case in which the LPCs are employed as the feature [3] is indicated by the yellow line. In addition, the case in which the FFT coefficients are employed [5] is indicated by the green dashed lines. It can be seen that the proposed method achieved the highest accuracy of 0.85 for running (M = 11) and 0.78 for walking (M = 9) among the three methods. The reason for this is considered to be that the proposed method employed simplified features compared with the LPCs and the FFT coefficients, and the individual difference was suppressed.

VI. Conclusion

A method for classifying the vibration sensor data into groups of children and adults was proposed. The magnitude and frequency of poles in the LP analysis are extracted as features and then fed to the LDA classifier. As the result of an experiment employing 40 subjects, a classification accuracy of approximately 80% was achieved. In future work, a method to adapt the model used in the proposed method to various environments should be addressed. The natural frequency of

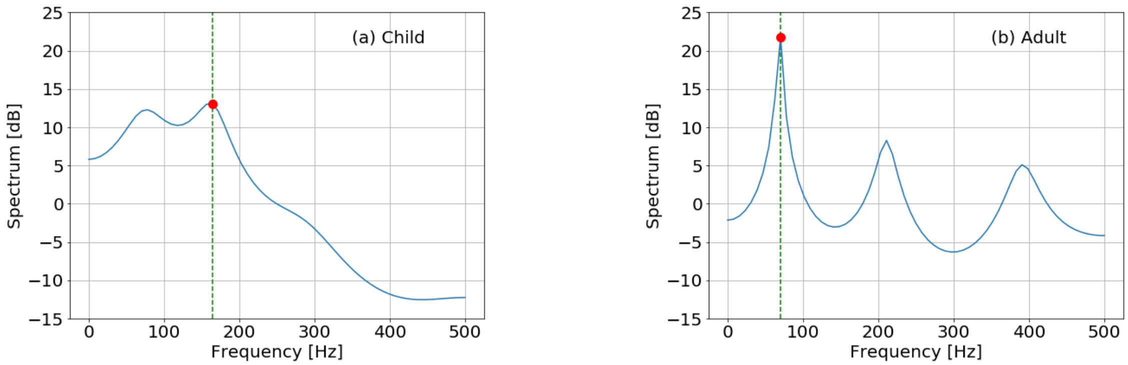

Fig. 5. Linear prediction spectrum for examples in the evaluation experiment described in Section V: (a) child and (b)adult.

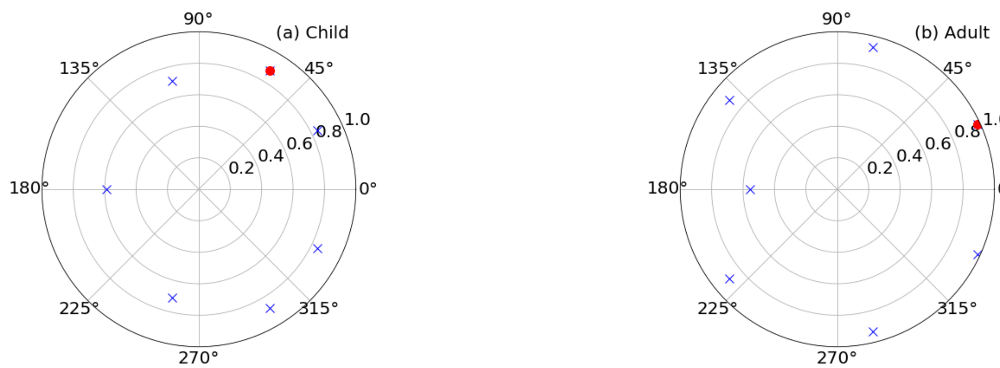

Fig. 6. Distribution of poles of the linear prediction transfer function for examples in the evaluation experiment described in Section V: (a) child and (b)adult. The red circle shows the pole with the largest radius.

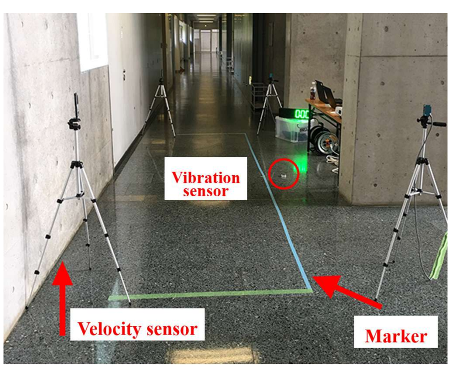

Fig. 7. Sensor configuration in the evaluation experiment.

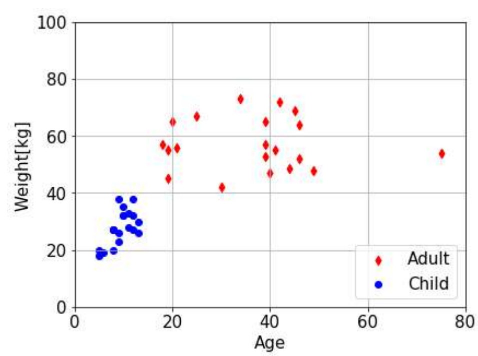

Fig. 8. Distribution of the ages and the weights of the subjects.

the floor can be obtained prior to the installation of the proposed system by a hammer striking test. By using the natural frequency data, the model used in the classification can be transformed so that it adapts to the environment. The case for multiple subjects should also be addressed.

References

[1] K. Ozaki, F. Asano, and K. Nakadai, "Estimation of the direction of footsteps using a single vibration sensor," *IEICE Trans. Fundamentals(Japanese Edition)*, vol. J101-A, no. 6, pp. 137–149, 2018.

[2] S. Tsubaki, F. Asano, and K. Nakadai, "Estimation of walking speed using a vibration sensor and multiple regression," submitted to SICE 2020, 2020.

[3] F. Asano and M. Fukushima, "Classification of foot- step attributes using a vibration sensor," in *Proc. APSIPA 2016*, 2016, p. Paper ID: 20.

[4] J. G. Proakis and D. G. Manolakis, *Digital Signal Processing (Third Edition)*, Prentice Hall, 1996.

[5] S. Pan, T. Yu, M. Mirshekari, J. Fagert, A. Bonde, O. J. Mengshoel, H. Y. Noh, and P. Zhang, "Footprintid: Indoor pedestrian identification through ambient structural vibration sensing," *Proceedings of the ACM*

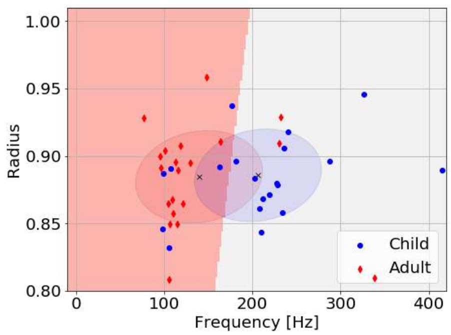

(a) Walking

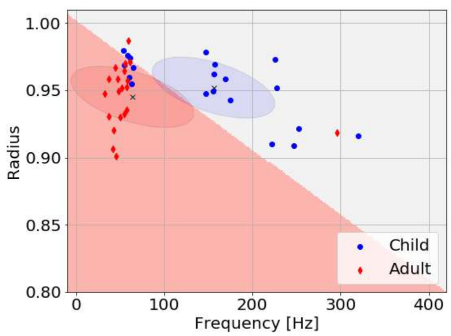

(b) Running

Fig. 9. Distribution of the features (radii and frequencies of poles).

on Interactive, Mobile, Wearable and Ubiquitous Technologies, vol. 1, no. 3, pp. Article 89, 2017.

[6] H. Fukai, Y. Mitsukura, and N. Hamad, “Image attribute class detection by using the emd,” in *IEICE Tech. Rep. (in Japanese)*, 2012, vol. 111 of *SIS2011-53*, pp. 1–4.

[7] H. John Pain and Patricia Rankin, *Introduction to Vibrations and Waves*, Wiley, 2015.

[8] C. Bishop, *Pattern recognition and machine learning*, Springer, 2006.

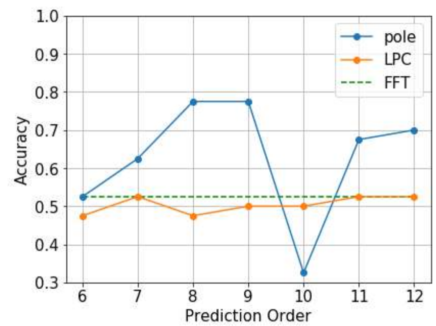

(a) Walking

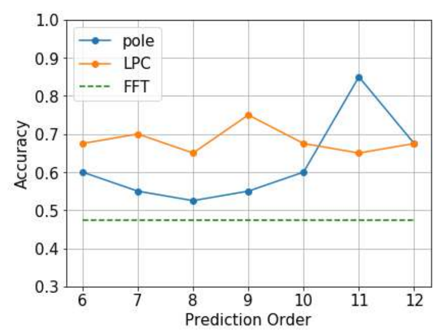

(b) Running

Fig. 10. Accuracy of the cross-validation test as a function of the prediction order M.